MARINE MANAGEMENT

Seasonal to multiannual marine ecosystem prediction with a global Earth system model

Jong-Yeon Park[1,2,3]*†, Charles A. Stock[2]†, John P. Dunne[2], Xiaosong Yang[2], Anthony Rosati[2]

Climate variations have a profound impact on marine ecosystems and the communities that depend upon them. Anticipating ecosystem shifts using global Earth system models (ESMs) could enable communities to adapt to climate fluctuations and contribute to long-term ecosystem resilience. We show that newly developed ESM-based marine biogeochemical predictions can skillfully predict satellite-derived seasonal to multiannual chlorophyll fluctuations in many regions. Prediction skill arises primarily from successfully simulating the chlorophyll response to the El Niño–Southern Oscillation and capturing the winter reemergence of subsurface nutrient anomalies in the extratropics, which subsequently affect spring and summer chlorophyll concentrations. Further investigations suggest that interannual fish-catch variations in selected large marine ecosystems can be anticipated from predicted chlorophyll and sea surface temperature anomalies. This result, together with high predictability for other marine-resource–relevant biogeochemical properties (e.g., oxygen, primary production), suggests a role for ESM-based marine biogeochemical predictions in dynamic marine resource management efforts.

The incorporation of biogeochemical processes into global climate models has transformed them into Earth system models (ESMs) that aspire to holistically represent the interacting physical, chemical, and biological processes shaping global carbon and nutrient cycles (*1*). Unlike physical climate models, ESMs can explore feedbacks between global change and carbon fluxes within and between terrestrial, ocean, and atmospheric reservoirs (*2*–*4*). For oceans, ESMs have further provided outlooks for marine-resource–relevant changes beyond warming, including ocean acidification, deoxygenation, and changing ocean productivity (*5*–*7*).

Although knowledge of potential multidecadal marine resource shifts associated with climate change is strategically vital, these trends underlie often irregular seasonal to interannual climate and marine resource variations. Failure to anticipate such fluctuations has been a major contributor to past fisheries collapses (*8*). The desire to sustain marine resources subject to climate-driven fluctuations and change has prompted efforts toward more dynamic, environmentally informed marine resource decisions (*9*), including integration of seasonal to multiannual physical climate forecasts into management frameworks (*10*–*12*). Whereas the reliability of physical predictors alone for anticipating marine ecosystem responses is often limited (*13*), recent observations and idealized modeling studies suggest that biogeochemical drivers (e.g., acidity, oxygen, primary production) may be more predictable than their physical counterparts (*14*).

The development of seasonal to interannual marine biogeochemical predictions has been impeded by diverse challenges. These include difficulties associated with the integration of biogeochemical models with ocean data-assimilation systems used for forecast initialization (*15*–*17*), uncertainty in both physical and biogeochemical model structure (*18*), limited availability of and difficulties associated with assimilating biogeochemical data (*19*, *20*), and the large computational cost of retrospective forecast experiments required to rigorously assess biogeochemical prediction skill. As a result, studies of global biogeochemical prediction have relied upon limited reforecast experiments and idealized configurations distinct from those used for operational seasonal to multiannual physical climate predictions (*14*, *21*).

In this study, we present results from 2-year global biogeochemical forecasts initialized on the first of each month between 1991 and 2017. Each prediction has 12 ensemble members, creating a database of nearly 4000 forecasts and 8000 simulation years. The prediction system was constructed by integrating the Carbon, Ocean Biogeochemistry and Lower Trophics (COBALT) marine biogeochemical model (*22*) with seasonal to multiannual climate predictions from the Geophysical Fluid Dynamics Laboratory's (GFDL) CM2.1 climate model (*23*). CM2.1 has been shown to skillfully recreate primary modes of natural climate variability (*24*) and has been applied extensively to study seasonal and multiannual climate prediction (*25*, *26*). The physical initialization for CM2.1 forecasts was based on GFDL's ensemble-coupled data assimilation (ECDA) system (*27*). For the biogeochemical initialization, COBALT was integrated with the data-assimilative ocean physics following a strategy that carefully avoids spurious vertical motions that can degrade biogeochemical simulations (*15*). This integration resulted in substantial reductions of biogeochemical biases relative to nonassimilative simulations (*15*, *22*). The resulting ocean-state estimate captures large-scale sea surface temperature (SST) and chlorophyll variations (figs. S1 to S4).

Predictions were assessed against 20 years of satellite-derived chlorophyll estimates (*28*), which offer a near-global, continuous, multidecade time series of ocean ecosystem anomalies. Chlorophyll has also been found to be a robust indicator of cross-ecosystem (*29*) and, in some places, interannual fish-catch variations (*30*). Ensemble mean predictions are drift corrected with a lead-dependent monthly forecast climatology from the 27-year ensemble mean forecasts (see the materials and methods in the supplementary materials for further details).

The global marine biogeochemical prediction system produces skillful chlorophyll predictions one season in advance in many ocean regions (Fig. 1A). Significant chlorophyll prediction skill above that of a persistence forecast extends beyond 1 year in some regions (Fig. 1, B to F, and fig. S5). Although skill varies by region and initialization month, characteristic patterns emerged for tropical and extratropical regions. In the tropical Pacific (Fig. 1B), prediction skill is limited to maximum leads of 12 months, with peak skill for fall/winter forecasts and reduced skill for boreal spring predictions. This pattern closely resembles the El Niño–Southern Oscillation (ENSO) SST prediction skill (fig. S6) and is consistent with prediction of ENSO-associated nutricline variations, which peak in boreal winter but have a weak boreal spring signal (*31*, *32*). Strong negative and positive winter chlorophyll anomalies are tightly linked to El Niño and La Niña events, respectively (Fig. 2A). This relationship also holds for the tropical Indian Ocean (Fig. 2B), which is subject to a lagged ENSO signal carried into the Indian Ocean through atmospheric teleconnections (*33*).

Chlorophyll predictions in extratropical systems are characterized by alternating predictable and unpredictable forecast windows (Fig. 1, D to F; note diagonal bands of alternating high- and low-anomaly correlation coefficients). In the subtropical to temperate North Atlantic (Fig. 1D), chlorophyll anomalies are not predictable in winter but are predictable during the productive spring, summer, and fall (i.e., the growing season). Furthermore, prediction skill remains evident through two growing seasons with leads up to 24 months. This skill results from successfully simulating the persistence of initial subsurface nutrient anomalies across seasons and successfully simulating the subsequent impact of these anomalies on surface chlorophyll. Winter nitrate (NO_3) anomalies linked to North Atlantic Oscillation (NAO)–driven wind anomalies (fig. S7)

[1]Atmospheric and Oceanic Sciences Program, Princeton University, Princeton, NJ 08540, USA. [2]National Oceanic and Atmospheric Administration/Geophysical Fluid Dynamics Laboratory, Princeton, NJ 08540, USA. [3]Department of Earth and Environmental Sciences, Chonbuk National University, Jeonju-si, Jeollabuk-do 54896, Republic of Korea.
*Corresponding author. Email: jongyeon.park@jbnu.ac.kr
†These authors contributed equally to this work.

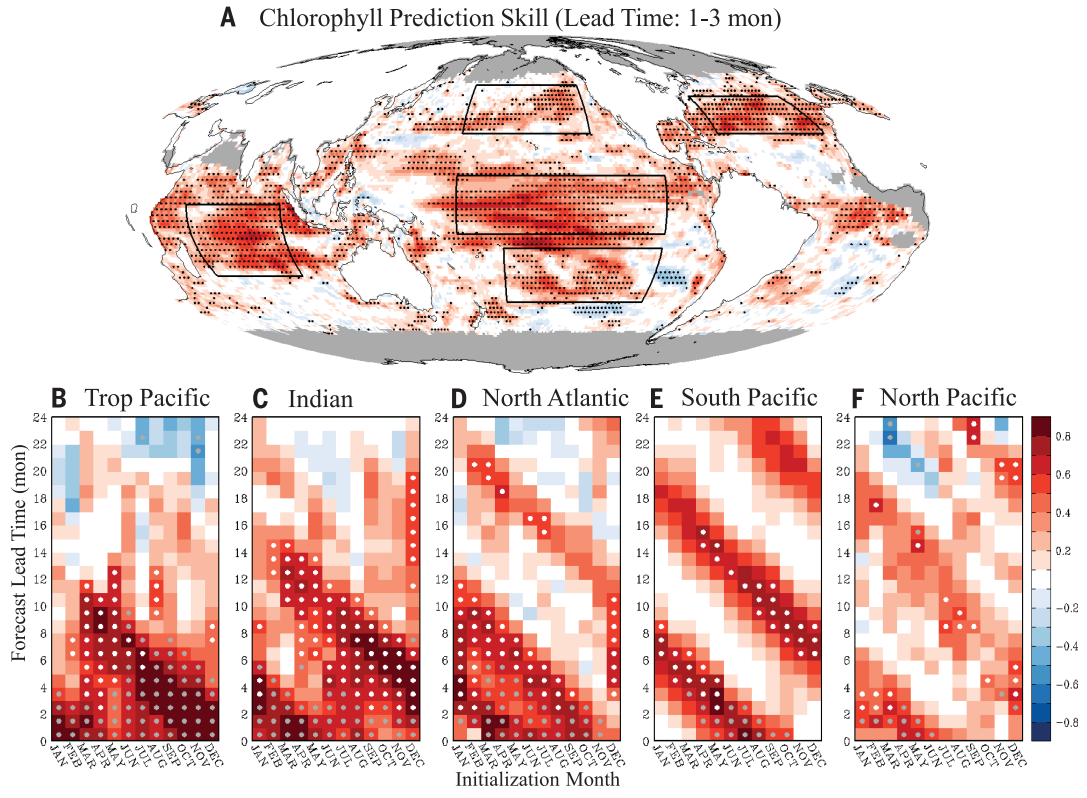

Fig. 1. Prediction skill in reproducing observed variations of monthly chlorophyll anomaly. (**A**) Chlorophyll prediction skill measured by the mean monthly anomaly correlation coefficient (ACC) between predicted and observed (satellite) chlorophyll at a 1- to 3-month lead time during the period 1997–2017. Stippled areas indicate that the correlation is significantly greater than 0 with 95% confidence. Areas with less than 80% satellite chlorophyll coverage are masked in gray. (**B** to **F**) Chlorophyll prediction skill as a function of forecast initialization month (*x* axis) and lead time (*y* axis) in the Tropical Pacific (170°E–100°W, 10°S–10°N), Indian (55°E–95°E, 25°S–0°S), North Atlantic (70°W–20°W, 25°N–40°N), North Pacific (170°E–130°W, 25°N–45°N), and South Pacific (170°W–100°W, 35°S–15°S) oceans. Circles indicate significant ($P < 0.05$) prediction skill: White circles indicate that the chlorophyll forecast skill from the biogeochemical prediction system exceeds the persistent forecast skill; gray circles indicate that the skill of the biogeochemical forecast is significant, but it is not significantly better than a persistence forecast. Three-month running mean anomalies are used for the calculation of ACCs.

remain evident beneath the mixed layer during summer and reemerge when the mixed layer deepens during the subsequent fall and winter (Fig. 3A). High-NO_3 anomalies then lead to elevated chlorophyll during the following growing season (Fig. 3B). A composite of high- versus low-chlorophyll years (fig. S8) confirms that high-NO_3 anomalies are associated with enhanced NO_3-based spring phytoplankton production, followed by enhanced ammonium-based (i.e., recycled) production during the summer and fall. This chlorophyll reemergence pattern resembles the mechanism for predicting midlatitude SST anomalies (*34*) but, unlike the predictable SST signal, which occurs after the breakdown of summer stratification, the predictable chlorophyll signal occurs during the stratified period.

Other extratropical areas exhibit variations on the basic reemergence mechanism illustrated for the North Atlantic. The South Pacific reemergence signal remains exceptionally strong through 2 years (Fig. 1E; Fig. 3, C and D; and fig. S9). In the North Pacific, prediction skill is weaker and limited in spatial extent (Fig. 1F; Fig. 3, E and F; and fig. S10). This may reflect a greater role of atmospheric iron deposition in the North Pacific masked by our current use of a constant deposition climatology (*22*) or stronger stochastic atmospheric forcing causing irregular and spatially less homogeneous chlorophyll fluctuations relative to other regions (*35*).

Successful prediction of chlorophyll anomalies in some regions across multiple years gives cause for optimism concerning the utility of biogeochemical predictions for marine resource application. As a proof of concept, we considered the capacity to anticipate interannual fluctuations in aggregate fish catch using predicted chlorophyll and SST, two known "bottom-up" drivers of fish catch (*12*, *29*, *30*). We assessed predictions in coastal large marine ecosystems (LMEs, fig. S11) accounting for over 95% of global fish catch (*36*). Annual mean fish-catch data were obtained from the Sea Around Us project (*37*). Despite coarse ocean grids that limit resolution of coastal circulation and ecosystem processes, global climate prediction systems have significant SST-forecasting skill for many LMEs (*38*, *39*), and our results show that this also holds for interannual chlorophyll anomalies (fig. S12).

We assessed the potential for biogeochemical predictions to inform interannual fish-catch fluctuations in a subset of LMEs based on three conditions. First, we identified LMEs in which past interannual catch fluctuations are significantly correlated with observed SST or chlorophyll anomalies over the retrospective forecast period. We considered both concurrent and 1-year–lagged relationships. The concurrent relationship tests for rapid catch responses such as immigration during favorable conditions. A 1-year lag allows for propagating environmental effects such as recruitment of short-lived species. Whereas longer lag responses between environmental drivers and ecosystem responses are possible (*40*, *41*), contemporaneous or short lag signals have proven to be the most tractable for management-driven forecasts (*42*) and are of primary interest for assessing the utility of the interannual biogeochemical predictions herein. Twenty-five out of the 54 heavily fished LMEs considered satisfied this first condition (Fig. 4 and figs. S13 and S14). The absence of a significant relationship in 29 LMEs does not imply that there are no "bottom-up" constraints on these systems, only that a relationship between interannual aggregate catch and SST or chlorophyll anomalies could not be discerned over the retrospective forecast period.

Second, we subselected LMEs for which the global biogeochemical prediction system could predict observed annual mean SST or chlorophyll anomalies with significant skill. Such cases were ubiquitous, with 38 of 54 LMEs satisfying this condition despite the model's coarse ocean resolution (fig. S12). Fifteen of these LMEs also satisfied our first condition (Fig. 4).

Third, we subselected LMEs in which the bottom-up relationship was strong enough and environmental predictions were skillful enough to significantly explain the reported aggregate interannual fish-catch anomalies. Consistent with our first selection condition, predicted

fish catch is based on a simple linear regression of catch anomalies against predicted environmental (SST, chlorophyll) anomalies with contemporaneous or 1-year–lagged relationships (see materials and methods). We focused on LMEs for which significant fish-catch relationships remained after detrending to reduce the potential of an erroneous attribution of fishing effort trends onto environmental factors. Six systems satisfied all three conditions (Fig. 4, table S1, and figs. S15 and S16): Gulf of Alaska, California Current, Humboldt Current, Canadian Eastern Arctic, Agulhas Current, and Somali Coastal Current systems (Fig. 4, lower panels). Four out of six LMEs exhibited significant fish-catch prediction skill for an additional year (i.e., at a 1- to 2-year lead time; Fig. 4, green lines).

In the Gulf of Alaska LME, catch fluctuations covaried with predictable coastal SST variations associated with the Pacific Decadal Oscillation, a basin-scale mode of climate variability with diverse fisheries links (*38*). In the California Current LME, the model predicts a recent observed chlorophyll increase off the Baja Peninsula that covaried with increased reported catch from this region (Fig. 4C). Weak ENSO imprints are also apparent, particularly a catch reduction after the 1997–1998 El Niño. This signal is more prominent in the Humboldt Current (Fig. 4D). In the Canadian Eastern Arctic LME, a predictable warming in the 1990s covaried with increasing northern prawn catches, both of which leveled off as temperatures stabilized in the 2000s (Fig. 4E). This LME is toward the cold-water end of the northern prawn range (*43*), suggesting a favorable response to warming. More complex interactions with changing plankton dynamics, however, cannot be ruled out (*43*).

In the Indian Ocean, increasing Agulhas LME catch between 1996 and 2004 corresponds to the increased prominence of the sardine fishery

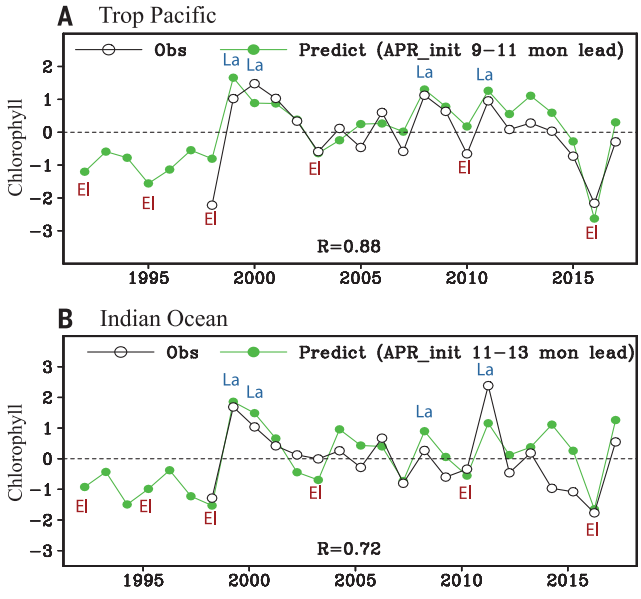

Fig. 2. Observed and predicted chlorophyll anomalies in the tropical oceans. (**A**) Observed (black) and predicted (green) wintertime (December-January-February) normalized chlorophyll anomalies in the tropical Pacific (170°E–100°W, 10°S–10°N). The predicted anomalies are 1 April–initialized chlorophyll predictions (i.e., forecast lead time is 9 to 11 months). (**B**) Similar to (A) but for 1 April–initialized springtime (February-March-April) chlorophyll anomalies in the Indian Ocean (55°E–95°E, 25°S–0°S; i.e., forecast lead time is 11 to 13 months). El Niño and La Niña years are marked with "El" and "La," respectively.

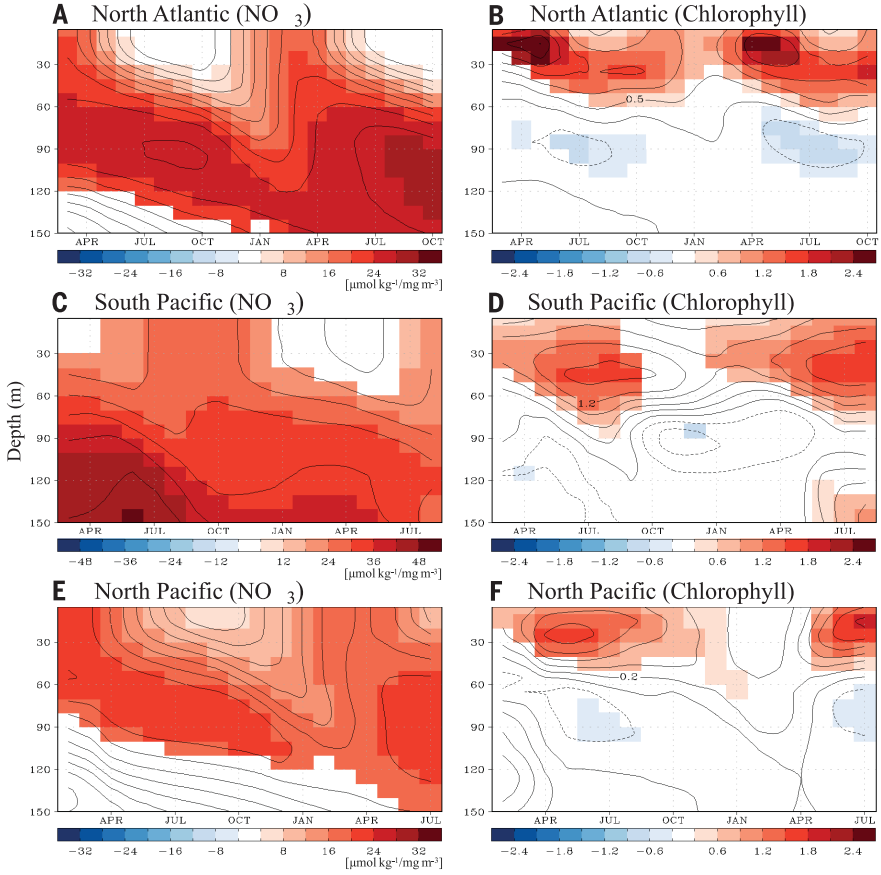

Fig. 3. Reemergence of subsurface biogeochemical anomalies linked to chlorophyll prediction skill in the extratropical oceans. (**A**) Temporal evolution of 1 March–initialized NO_3 anomaly prediction in the North Atlantic Ocean (70°W–20°W, 25°N–40°N). NO_3 anomalies are regressed onto predicted SON (September-October-November) surface chlorophyll concentrations during the following year. That is, positive values indicate that elevated NO_3 at the specified time and depth are associated with elevated SON chlorophyll 18 to 21 months after the initialization. The anomalies are 3-month running means. (**B**) Similar to (A) but for 1 March–initialized chlorophyll anomaly prediction. (**C**) and (**D**) are similar to (A) and (B), respectively, but for 1 March–initialized prediction in the south Pacific (170°W–100°W, 35°S–15°S) regressed onto 1 March–initialized July-August-September chlorophyll prediction of the following year. (**E**) and (**F**) are similar to (**A**) and (**B**), respectively, but for 1 February–initialized prediction in the North Pacific (170°E–130°W, 25°N–45°N) regressed onto 1 February–initialized June-July-August chlorophyll prediction of the following year. Shaded areas represent the 95% confidence region.

(*44*). Although debate over the cause of this increase remains, its consistency with a lagged chlorophyll relationship is suggestive of a recruitment link. Catch variations in the neighboring Somali Coastal Current are similar to those in the Agulhas, but the underlying characteristics of chlorophyll predictability are different. Agulhas anomalies follow a midlatitude reemergence pattern similar to that of the extratropical areas shown in Fig. 1, whereas the Somali system exhibits relatively limited chlorophyll prediction skill because of equatorial waves repeatedly triggered by ENSO and the Indian Ocean dipole (fig. S17) (*45*). In both the Agulhas and Somali systems, annual fish catch was predictable up to 2 to 3 years in advance using the 1-year–lagged relationship between catch and chlorophyll.

Although only six LMEs met the most stringent criteria for skillful prediction of interannual catch anomalies from SST or chlorophyll, many notable relationships for individual climate-sensitive fish stocks may underlie aggregate catch relationships (fig. S18). More detailed accounting for fish-stock dynamics (*42*) and variations in fishing effort could also better isolate predictable bottom-up signals (*30*). The prediction skill threshold at which forecasts become useful is fishery dependent, but recent management strategy evaluations suggest an elevated likelihood of utility for species with short prerecruit survival windows or strong environmental bottlenecks (*12*, *42*). In addition, biogeochemical prediction systems can extend beyond SST and chlorophyll to include other potential drivers, including oxygen, acidity, net primary production (NPP), and zooplankton. Assessment of NPP predictions

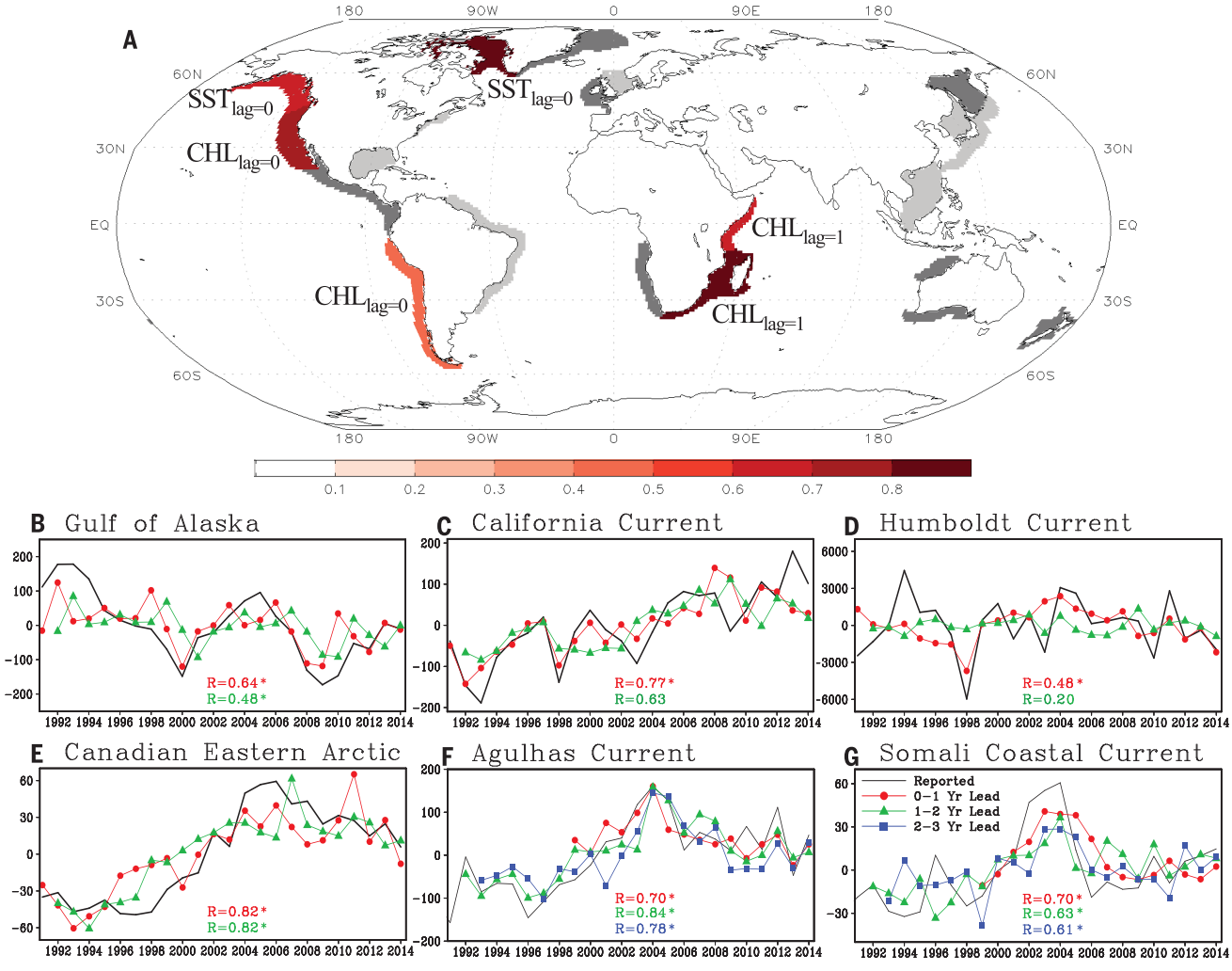

Fig. 4. Potential utility of marine biogeochemistry prediction for annual fish-catch prediction. (**A**) All shaded LMEs represent regions where past annual fish-catch fluctuations are significantly correlated with observed bottom-up factors [i.e., SST or chlorophyll (CHL)]. Dark gray represents regions where the ESM-based prediction system can predict bottom-up forcing changes, and color shadings represent regions where the ESM-based prediction system can predict both bottom-up forcing changes and reported fish catch. Bottom-up factors and the time lag used for fish-catch predictions are shown near each predictable LME. (**B** to **G**) Reported (black lines) and predicted (colored lines) annual mean fish catches in (B) Gulf of Alaska, (C) California Current, (D) Humboldt Current, (E) Canadian Eastern Arctic, (F) Agulhas Current, and (G) Somali Coastal Current LMEs (unit: 10^3 tonnage). Predicted annual fish catches are based on the 1 January–initialized SST (for the Gulf of Alaska and Canadian Eastern Arctic systems) or chlorophyll (for other systems) predictions in the coming year (i.e., forecast lead time is 0 to 1 year; red lines) and the following year (i.e., forecast lead time is 1 to 2 years; green lines). In each LME, the time lag at which the maximum fish-catch prediction skill occurs is used for the fish-catch prediction. For example, the fish-catch predictor for Agulhas Current is the annual mean chlorophyll in the previous year, thus the observed annual mean chlorophyll in the previous year is used for the 0- to 1-year lead-time forecast. Similarly, 1 January–initialized chlorophyll predictions for the coming and following years are used for the 1- to 2-year and 2- to 3-year lead-time forecasts in the Agulhas Current system. Asterisks indicate the significant ($P < 0.05$) correlation between reported and predicted annual fish catches.

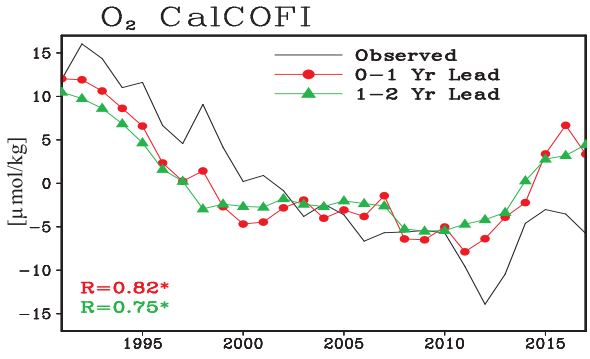

Fig. 5. Oxygen prediction in the California Current LME as an example of extension to other biogeochemical stressor properties. Observed oxygen from the California Cooperative Fisheries Investigations (CalCOFI) program (black lines) and 1 January–initialized oxygen prediction for the coming year (0- to 1-year lead time; red line) and for the following year (1- to 2-year lead time; green line). Dissolved oxygen shown here is the averaged value between the 200- and 500-m depth in the CalCOFI region. Asterisks indicate a significant ($P < 0.05$) correlation between observed and predicted oxygen.

against satellite-based NPP algorithms suggests patterns of predictability similar to those of chlorophyll (fig. S19), whereas model-based assessments of the potential predictability of other drivers suggest that they may be more predictable than chlorophyll or SST (fig. S20). For example, subsurface oxygen predictions that accompany the skillful California Current LME chlorophyll predictions highlighted in Fig. 4 were robust throughout our 2-year prediction horizon (Fig. 5). Such lasting and predictable "biogeochemical memory" gives cause for further optimism concerning the benefit of extending physical climate predictions to marine biogeochemical predictions for marine resource management in a dynamic environment.

REFERENCES AND NOTES

1. G. B. Bonan, S. C. Doney, *Science* **359**, eaam8328 (2018).
2. P. Friedlingstein *et al.*, *J. Clim.* **27**, 511–526 (2014).
3. A. Anav *et al.*, *J. Clim.* **26**, 6801–6843 (2013).
4. J. L. Sarmiento, T. M. C. Hughes, R. J. Stouffer, S. Manabe, *Nature* **393**, 245–249 (1998).
5. W. W. L. Cheung *et al.*, *ICES J. Mar. Sci.* **73**, 1283–1296 (2016).
6. C. A. Stock *et al.*, *Proc. Natl. Acad. Sci. U.S.A.* **114**, E1441–E1449 (2017).
7. L. Bopp *et al.*, *Biogeosciences* **10**, 6225–6245 (2013).
8. F. P. Chavez, J. Ryan, S. E. Lluch-Cota, C. M. Niquen, *Science* **299**, 217–221 (2003).
9. K. N. Marshall, L. E. Koehn, P. S. Levin, T. E. Essington, O. P. Jensen, *ICES J. Mar. Sci.* **76**, 1–9 (2019).
10. A. J. Hobday, C. M. Spillman, J. P. Eveson, J. R. Hartog, *Fish. Oceanogr.* **25**, 45–56 (2016).
11. D. Tommasi *et al.*, *Prog. Oceanogr.* **152**, 15–49 (2017).
12. D. Tommasi *et al.*, *Ecol. Appl.* **27**, 378–388 (2017).
13. R. A. Myers, *Rev. Fish Biol. Fish.* **8**, 285–305 (1998).
14. R. Séférian *et al.*, *Proc. Natl. Acad. Sci. U.S.A.* **111**, 11646–11651 (2014).
15. J. Y. Park *et al.*, *J. Adv. Model. Earth Syst.* **10**, 891–906 (2018).
16. K. Raghukumar *et al.*, *Prog. Oceanogr.* **138**, 546–558 (2015).
17. J. Waters, M. J. Bell, M. J. Martin, D. J. Lea, *QJRMS* **143**, 195–208 (2017).
18. E. Hawkins, R. S. Smith, J. M. Gregory, D. A. Stainforth, *Clim. Dyn.* **46**, 3807–3819 (2016).
19. D. A. Ford *et al.*, *Ocean Sci.* **8**, 751–771 (2012).
20. H. Song, C. A. Edwards, A. M. Moore, J. Fiechter, *Ocean Model.* **106**, 131–145 (2016).
21. C. S. Rousseaux, W. W. Gregg, *Front. Mar. Sci.* **4**, 236 (2017).
22. C. A. Stock, J. P. Dunne, J. G. John, *Prog. Oceanogr.* **120**, 1–28 (2014).
23. T. L. Delworth *et al.*, *J. Clim.* **19**, 643–674 (2006).
24. A. T. Wittenberg, A. Rosati, N. C. Lau, J. J. Ploshay, *J. Clim.* **19**, 698–722 (2006).
25. B. P. Kirtman *et al.*, *Bull. Am. Meteorol. Soc.* **95**, 585–601 (2014).
26. G. A. Meehl *et al.*, *Bull. Am. Meteorol. Soc.* **95**, 243–267 (2014).
27. S. Zhang, M. J. Harrison, A. Rosati, A. Wittenberg, *Mon. Weather Rev.* **135**, 3541–3564 (2007).
28. NASA Goddard Space Flight Center, Ocean Ecology Laboratory, Ocean Biology Processing Group, Moderate-resolution Imaging Spectroradiometer (MODIS) Terra Aqua Chlorophyll Data (NASA OB.DAAC, 2014).
29. K. D. Friedland *et al.*, *PLOS ONE* **7**, e28945 (2012).
30. C. J. McOwen, W. W. L. Cheung, R. R. Rykaczewski, R. A. Watson, L. J. Wood, *Fish Fish.* **16**, 623–632 (2015).
31. M. J. Behrenfeld *et al.*, *Science* **291**, 2594–2597 (2001).
32. F. P. Chavez *et al.*, *Science* **286**, 2126–2131 (1999).
33. S. Venzke, M. Latif, A. Villwock, *J. Clim.* **13**, 1371–1383 (2000).
34. M. A. Alexander, C. Deser, M. S. Timlin, *J. Clim.* **12**, 2419–2433 (1999).
35. A. Morel, H. Claustre, B. Gentili, *Biogeosciences* **7**, 3139–3151 (2010).
36. K. Sherman, in *Sustaining Large Marine Ecosystems: The Human Dimension*, T. M. Hennessey, J. G. Sutinen, Eds. (2005), vol. 13, pp. 3–16.
37. D. Pauly, D. Zeller, *Nat. Commun.* **7**, 10244 (2016).
38. C. A. Stock *et al.*, *Prog. Oceanogr.* **137**, 219–236 (2015).
39. D. Tommasi *et al.*, *Front. Mar. Sci.* **4**, 201 (2017).
40. E. Di Lorenzo, M. D. Ohman, *Proc. Natl. Acad. Sci. U.S.A.* **110**, 2496–2499 (2013).
41. P. Le Mezo *et al.*, *J. Mar. Syst.* **153**, 55–66 (2016).
42. M. Haltuch *et al.*, *Fish. Res.* **217**, 198–216 (2019).
43. P. Koeller *et al.*, *Science* **324**, 791–793 (2009).
44. L. Hutchings *et al.*, *Prog. Oceanogr.* **83**, 15–32 (2009).
45. J. Currie *et al.*, *Biogeosciences* **10**, 6677–6698 (2013).

ACKNOWLEDGMENTS

We thank the anonymous reviewers for helpful and constructive comments on the manuscript. We also thank T. Delworth and F. Gonzalez-Taboada for internal reviews of the manuscript and J. Link, R. Watson, and V. Lam for discussions and input during the revision process. **Funding:** This work was supported by NOAA's marine ecosystem tipping points initiative. J.-Y.P. was also supported by the National Research Foundation of Korea (grant NRF-2018R1C1B5086584). **Author contributions**: J.-Y.P., C.A.S., J.P.D, X.Y., and A.R. conceived the experiments. J.-Y.P. and C.A.S. wrote the manuscript. J.-Y.P. performed experiments with X.Y. and analyzed the data. All authors discussed the results and commented on the manuscript at all stages. **Competing interests**: The authors declare no competing interests. **Data and materials availability**: The model simulation data used here are archived at NOAA's Geophysical Fluid Dynamics Laboratory (GFDL) server. Complete datasets may be requested from J.-Y.P. Key data used in the main manuscript and supplementary materials are archived at GFDL's public server (ftp://nomads.gfdl.noaa.gov/users/Jong-Yeon.Park/ESMprediction/).

SUPPLEMENTARY MATERIALS

science.sciencemag.org/content/365/6450/284/suppl/DC1
Materials and Methods
Table S1
Figs. S1 to S20
References (*46*–*54*)

8 October 2018; accepted 25 June 2019
10.1126/science.aav6634